Planta (2011) 233:123–137
DOI 10.1007/s00425-010-1284-9

ORIGINAL ARTICLE

Molecular characterization of a miraculin-like gene differentially expressed during coffee development and coffee leaf miner infestation

Jorge Maurício Costa Mondego · Melina Pasini Duarte · Eduardo Kiyota · Leandro Martínez · Sandra Rodrigues de Camargo · Fernanda P. De Caroli · Beatriz Santos Capela Alves · Sandra Maria Carmello Guerreiro · Maria Luiza Vilela Oliva · Oliveiro Guerreiro-Filho · Marcelo Menossi

Received: 13 August 2010 / Accepted: 15 September 2010 / Published online: 8 October 2010

Abstract The characterization of a coffee gene encoding a protein similar to miraculin-like proteins, which are members of the plant Kunitz serine trypsin inhibitor (STI) family of proteinase inhibitors (PIs), is described. PIs are important proteins in plant defence against insects and in the regulation of proteolysis during plant development. This gene has high identity with the Richadella dulcifica taste-modifying protein miraculin and with the tomato protein LeMir; and was named as CoMir (Coffea miraculin). Structural protein modelling indicated that CoMir had structural similarities with the Kunitz STI proteins, but suggested specific folding structures. CoMir was up-regulated after coffee leaf miner (Leucoptera coffeella) oviposition in resistant plants of a progeny derived from crosses between C. racemosa (resistant) and C. arabica (susceptible). Interestingly, this gene was down-regulated during coffee leaf miner herbivory in susceptible plants. CoMir expression was up-regulated after abscisic acid application and wounding stress and was prominent during the early stages of flower and fruit development. In situ hybridization revealed that CoMir transcripts accumulated in the anther tissues that display programmed cell death (tapetum, endothecium and stomium) and in the metaxylem vessels of the petals, stigma and leaves. In addition, the recombinant protein CoMir shows inhibitory activity against trypsin.

Electronic supplementary material The online version of this article (doi:10.1007/s00425-010-1284-9) contains supplementary material, which is available to authorized users.

J. M. C. Mondego · M. P. Duarte · S. R. de Camargo · M. Menossi
Laboratório de Genoma Funcional Departamento de Genética, Evolução e Bioagentes, Instituto de Biologia, Universidade Estadual de Campinas (UNICAMP), CP 6109, Campinas, SP 13084-971, Brazil

E. Kiyota
Centro de Biologia Molecular e Engenharia Genética, Universidade Estadual de Campinas (UNICAMP), CP 6010, Campinas, SP 13083-875, Brazil

E. Kiyota
Instituto de Química, Universidade Estadual de Campinas (UNICAMP), CP 6154, Campinas, SP 13084-862, Brazil

L. Martínez
Instituto de Física de São Carlos, Universidade de São Paulo (USP), Grupo de Cristalografia, CP 369, São Carlos, SP 13566-590, Brazil

F. P. De Caroli · M. L. V. Oliva
Departamento de Bioquímica, Universidade Federal de São Paulo (UNIFESP), São Paulo, SP 04044-020, Brazil

B. S. C. Alves
Laboratório Nacional de Biociências (LNBio), CP 6192, Campinas, SP 13083-970, Brazil

S. M. C. Guerreiro
Departamento de Biologia Vegetal, Instituto de Biologia, Universidade Estadual de Campinas (UNICAMP), CP 6109, Campinas, SP 13084-971, Brazil

O. Guerreiro-Filho
Centro de Café Alcides Carvalho, Instituto Agronômico de Campinas (IAC), Campinas, SP 13012-970, Brazil

J. M. C. Mondego (✉)
Centro de Pesquisa e Desenvolvimento de Recursos Genéticos Vegetais, Instituto Agronômico de Campinas (IAC), CP 28, Campinas, SP 13001-970, Brazil
e-mail: jmcmondego@iac.sp.gov.br; jmcmondego@gmail.com

According to the present results CoMir may act in proteolytic regulation during coffee development and in the defence against *L. coffeella*. The similarity of CoMir with other Kunitz STI proteins and the role of *CoMir* in plant development and plant stress are discussed.

Keywords Coffee · Kunitz STI proteinase inhibitor · Miraculin- like protein · Plant-insect interaction · Xylem · Programmed cell death

Abbreviations

BAPA	Nα-Benzoyl-D, L-Arginin-p-nitroanilid
CV	Column volume
IMAC	Immobilized metal affinity chromatography
MLP	Miraculin-like protein
PI	Proteinase inhibitor
STI	Soybean trypsin inhibitor
RACE	Rapid amplification of cDNA end

Introduction

Proteinase inhibitors (PIs) are ubiquitous proteins that bind to proteinases, blocking proteolysis of the target substrate (Laskowski and Kato 1980). Plants produce serine PIs in response to insect feeding. These proteins can arrest insect development by inhibiting digestive proteinases (Rodrigues-Macedo et al. 2003; Sumikawa et al. 2010), which are key proteins in the growth and reproductive success of arthropods (Murdock and Shade 2002). PIs are also involved in plant homeostasis by regulating the activity of endogenous proteases. Evidence points to the participation of PIs in drought stress resistance (Huang et al. 2007), in the regulation of proteolysis during seed germination (Jones and Fontanini 2003) and in the development of the phloem (Xu et al. 2001) and xylem (Jiménez et al. 2007). Proteolysis is observed during programmed cell death (PCD), an active and controlled cell suicide that occurs in xylem differentiation, during seed and flower development and during hypersensitive response (HR) to pathogens (van Doorn and Woltering 2005). Thus, there is growing evidence that PIs may act as regulators of PCD.

Proteins of the Kunitz STI family of serine PIs (MEROPS proteinase inhibitor family I3A, Rawlings et al. 2004) contain a conserved signature in the N-terminal region [(L/I/V/M)-x-D-x-(E/D/N/T/Y)-(D/G)-(R/K/H/D/E/N/Q)-x-(L/I/V/M)-x-(5)-Y-(L/I/V/M)], 12 conserved β-strands classified as three groups of four sheets each, forming a β-trefoil structure (McLachlan 1979) and a reactive site between β-sheets A4 and B1.These proteins frequently contain two conserved disulfide bridges, with the exception of some Kunitz STI from *Bauhinia* spp that have only one or no disulfide bridges (Hansen et al. 2007; Oliva and Sampaio 2008) and miraculin-like proteins (MLPs) that contain three disulfide bridges (Gahloth et al. 2010). Miraculin is a taste-modifying protein, extracted from the African shrub *Richadella dulcifica* (Theerasilp and Kurihara 1988). MLPs are supposed to exert functions during the biotic stress responses of plants. For instance, the MLP tumour-related protein NF34 elicited HR in the tobacco mosaic virus (TMV)-susceptible tobacco plants when over-expressed by a TMV expression vector (Karrer et al. 1998); LeMir, a tomato MLP, was induced early after infection of the tomato with the root-knot nematodes *Meloidogyne javanica* (Brenner et al. 1998); and a rough lemon MLP showed anti-fungal activity against *Alternaria citri* (Tsukuda et al. 2006).

Coffee is the second most important commodity in the world. *Coffea arabica*, the main cultivated species, is susceptible to infestation by the coffee leaf miner (*Leucoptera coffeella*) (Guérin Méneville, Lepidoptera: Lyonetiidae) (Guerreiro-Filho et al. 1999). To evaluate the molecular mechanisms of resistance against *L. coffeella*, plants of a hybrid progeny derived from crosses between *C. arabica* and *C. racemosa* (a species naturally resistant to *L. coffeella*) were infested, and RNA from the different treatments was used to construct a subtracted cDNA library enriched with genes induced during leaf miner attack (Mondego et al. 2005). Twenty-one cDNA clones were differentially expressed during infestation. One of them, SSH101B04, was similar to a MLP.

In the present report, the cloning and characterization of a *MLP* gene from coffee is described. Due to its similarity to tomato *LeMir*, this gene was named *CoMir*. The *CoMir* expression was assessed during coffee development and after the application of abscisic acid (ABA), wounding stress and coffee leaf miner infestation. The subcellular localization, structural modelling and anti-proteolytic activity of the CoMir protein were also evaluated. Possible functions of *CoMir* in plant stress and development and the putative CoMir structural characteristics are discussed.

Materials and methods

Insect rearing and plant material

Leucoptera coffeella moths were reared according to Guerreiro-Filho et al. (1991). Coffee plants were obtained from the Campinas Agronomic Institute (IAC, Campinas, Brazil). Plants from the progeny H14954-29 from the fifth backcross generation of the [(*C. racemosa* × *C. arabica*) × *C. arabica*] breeding program were used for leaf miner infestation and Southern-blot analysis. Ten-year-old *C. arabica* cultivar Mundo Novo plants were used to assess

the *CoMir* organ-specific expression and *CoMir* expression after applying methyl-jasmonate (MeJA), abscisic acid (ABA) and wounding treatments. The first pair of leaves, roots, different phases of flower development (green flower bud, white flower bud and open flower) and coffee fruits at different stages of development (early green, green, green-yellow, yellow, yellow-red and red) were collected and frozen in liquid nitrogen for the RNA blot analysis (see below). For in situ hybridization, leaf discs, green flower buds and white flower buds were collected and incubated in tissue fixative (see below). Plants were grown in a controlled environment at 26 ± 1°C with a photoperiod of approximately 16 h light.

Coffee leaf miner infestation

Infestation experiments were carried out as described elsewhere (Mondego et al. 2005). Briefly, young leaves from highly resistant plants (R) and highly susceptible plants (S) were detached and inserted by the petiole into 2-ml microcentrifuge tubes previously filled with water, which were placed into plastic supports. 40 R and 40 S leaves were placed in *L. coffeella* rearing cages and concomitantly, 20 R and 20 S leaves were incubated in a plastic box without *L. coffeella* moths. Leaf discs with eggs or with mines on the leaf surface were collected using 3–8 cm diameter cork borers and immediately frozen in liquid nitrogen after collection. 72 h after infestation, *L. coffeella* eggs were removed from 20 R leaves (Ro: resistant after oviposition) and 20 S leaves (So: susceptible after oviposition) and the respective leaf discs collected. 96 h after Ro/So collection (i.e. after egg hatching), the larvae were removed from the mines of the remaining 20 R leaves (Re: resistant after larval eclosion) and 20 S leaves (Se: resistant after eclosion) and leaf discs were collected. Leaf discs from control S (Sc: susceptible control) and control R (resistant control) leaves were also collected. All leaf discs were immediately frozen in liquid nitrogen after collection.

Wounding, abscisic acid and methyl jasmonate treatments

For the wounding treatment, the first pair of leaves was wounded using the method of Reymond et al. (2000) with modifications. Briefly, leaves were wounded in six places (including secondary veins) using a forceps, which damaged approximately 50% of the leaf surface. For the abscisic acid (ABA) and methyl jasmonate (MeJA) treatments, the plants were sprayed with 100 μM solutions. After treatment, the plants were incubated for 1, 4, 12 and 24 h in an acclimated chamber (26°C) with constant light. At each time point, leaves were harvested and immediately frozen in liquid nitrogen.

Amplification and cloning

The DNA sequences of the clones SSH101B04 (Mondego et al. 2005) and SSH104C02 (which overlaps with SSH101B04) were used to design primers. 5′ RACE amplifications were performed using the version 2.0 5′ RACE System (Invitrogen, Carlsbad, CA, USA) using *CoMir* 3′NTR as the template for a gene-specific primer design: 5′ CTCCTTATTGTGCTTGCTTAA 3′ (primer #1). cDNA was synthesized from RNA extracted from resistant plants after coffee leaf miner oviposition (Mondego et al. 2005). Platinum HiFi *Taq* DNA polymerase (Invitrogen) was used according to the manufacturer's instructions. The single RACE product was isolated from agarose gel using a GFX purification kit (GE Healthcare, Little Chalfont, UK) and cloned into the plasmid pGEM T-Easy (Promega, Madison, WI, USA). For further cloning, this construct was used as the template in PCR using the following primers: 5′ CCATGGCAATGAAGAAATTACTTCTCTTCCTTT 3′ (primer #2) and 5′ *GGATCC*CAAAGTAGAGGTAACGG ACTTGAGAA 3′ (primer #3). The single PCR band was cloned in pGEM T-easy, originating the pGEMCoMir plasmid. For amplification of *CoMir* without the signal sequence, the same construction used as the template in PCR was used, using primer #4 (5′ CCATGGAGTATCCAGT GCTCGACATCAA) and primer #3. The resulting fragment was cloned in pGEM T-easy, resulting in the pGEM-CoMirSS plasmid. Underlined and italics sequences correspond to the *Nco*I and *Bam*HI sites, respectively.

DNA extraction and Southern-blot analysis

Coffee leaves were ground in liquid nitrogen and 0.2 g of tissue was resuspended in 1.5 ml of lysis buffer (0.35 M sorbitol; 0.1 M Tris–HCl pH 8.0; 50 mM EDTA, pH 8.0; 1.5% β-mercaptoethanol, v/v). The supernatant was discarded and the pellet resuspended in 370 μl of lysis buffer, 520 μl of extraction buffer (0.2 M Tris–HCl pH 8.0; 50 mM EDTA pH 8.0; 2 M NaCl; 2% CTAB w/v) and 110 μl of 10% SDS. The samples were incubated for 40 min at 65°C in a water bath, mixing every 10 min. After 10 min at room temperature, chloroform/isoamyl-alcohol (24:1, v:v) was added and the samples centrifuged. The aqueous phase was recovered and the DNA precipitated with 3 M sodium acetate pH 5.2 (0.1 v) and cooled isopropanol (1 v) at −20°C for 2 h. After centrifugation, the pellet was resuspended in 200 μl of water and treated with 200 μg/ml of RNAse A (Calbiochem, EMD, Gibbstown, NJ, USA) for 30 min at 37°C. Eight hundred microlitres of water and 1 ml of phenol:chloroform:isoamyl-alcohol (25:24:1, by vol.) were then added to the sample, the tubes centrifuged and the aqueous phase recovered. The DNA was precipitated with 3 M sodium acetate pH 5.2 (0.15 v) and cooled isopropanol

(0.8 v) at −20°C for 16 h. After centrifugation, the supernatant was discarded and the pellets washed in 70% ethanol and resuspended in water. Ten micrograms of DNA was digested with 50 units of *Eco*RI and *Eco*RV restriction enzymes (Fermentas Life Sciences,Vilnius, Lithuania) at 37°C for 16 h and the digested DNA loaded and fractionated in 1.2% (w/v) agarose gel. Subsequently, the gel was treated with 0.25 M HCl for 10 min, with denaturing buffer (0.4 M NaOH and 0.6 M NaCl) for 1 h and with neutralizing buffer (1.5 M NaCl and 1 M Tris–HCl pH 7.5) for 1 h. After rinsing in water, the gel was transferred to a Hybond-N+ filter (GE Healthcare). The membrane was hybridized at 42°C with *CoMir* insert labelled with [α-^{32}P] dCTP (Sambrook et al.1989) and washed twice for 10 min each in a solution containing 1× SSC and 0.1% SDS at 42°C and subsequently twice more for 10 min each in 0.1× SSC and 0.1% SDS at 42°C. The membranes were sealed in plastic and exposed to imaging plates (Fujifilm, Tokyo, Japan) and the digitalized images quantified using Image Gauge Software (Fujifilm).

RNA extraction and RNA blot

RNA extraction was performed as described elsewhere (Mondego et al. 2005). Ten micrograms of total RNA was incubated in denaturing RNA buffer for 15 min at 56°C and then fractionated in a 1% (w/v) agarose gel containing formaldehyde. The gel was subsequently blotted onto a Hybond-N+ filter (GE Healthcare), the filters hybridized at 42°C with *CoMir* insert labelled with [α-^{32}P] dCTP (Sambrook et al. 1989) for 16 h, and then washed in a solution containing 0.2× SSC and 0.1% SDS at room temperature for 20 min and finally in 0.2× SSC and 0.1% SDS at 42°C for 20 min. The membranes were sealed in plastic and exposed to imaging plates (Fujifilm) and the digitalized images quantified using Image Gauge Software (Fujifilm).

Subcellular localization

pGEMCoMir was digested with *Nco*I and *Spe*I (Invitrogen), liberating the *CoMir* insert. This DNA fragment was ligated into pCAMBIA 1302 (Cambia, Brisbane, Australia) downstream of the CaMV 35S promoter and fused in frame upstream of the green fluorescent protein (mGFP5) reporter gene (Haseloff 1999). Onion (*Allium cepa* L.) epidermal cells were transiently transformed with the *CoMir::mGFP5* construct, using a helium biolistic gene transformation system (Embrapa, Brasilia, Brazil). Five micrograms of plasmid DNA, dialysed against water, was precipitated using 1.6 mm gold particles (Bio-Rad, Hercules, CA, USA), 2.5 M $CaCl_2$ and 0.1 M spermidine. The inner epidermal cell layers were peeled from the onion, placed on MS solid medium (Murashige and Skoog 1962) and bombarded with ethanol resuspended DNA-coated particles at 1,300 psi. The tissues were subsequently incubated for 24 h in the dark at 22°C and plasmolysed on glass slides containing a 20% (w/v) sucrose solution. The fusion constructs were detected by GFP fluorescence at 508 nm using a Nikon Eclipse E600 microscope (Nikon, Tokyo, Japan). Bright field and fluorescence images were photographed and digitalized using Image Pro Plus program (Media Cybernetics, Bethesda, MD, USA).

In situ hybridization

The pGEMCoMir plasmid was linearized with appropriate enzymes and used as a template for in vitro transcription according to the digoxigenin RNA labelling Kit (Roche, Mannheim, Germany). Antisense and sense riboprobes were then sheared by alkaline hydrolysis to an average size of 250 bp. The plant material was vacuum-infiltrated with FAA solution (10% formaldehyde, 50% ethanol, 5% acetic acid), the tissue dehydrated in an ethanol and xylene graded series and embedded in paraffin (Histosec®, Merck, Darmstadt, Germany). For hybridization, 10-µm-thick sections were positioned on Probe On Plus™ slides (Fisher Scientific, Pittsburgh, PA, USA), hydrated and treated with 20 µg/ml of proteinase K (Invitrogen) for 15 min at 37°C. The slides were incubated in PBS (16 mM NaH_2PO_4, 84 mM Na_2HPO_4, 1.5 M NaCl) for 2 min, in 0.2% glycine in PBS for 2 min and in 4% paraformaldehyde in PBS for 20 min. Subsequently, the slides were equilibrated in a solution containing 0.1 M triethalonamine pH 8.0 and 0.1% acetic anhydride for 10 min, washed in PBS and gradually dehydrated. Hybridization with riboprobes was carried out at 50°C for 16 h in 50% formamide, 5× SSC, 5% SDS, 100 µg/ml tRNA, 100 µg/ml poli-A and 500 ng of riboprobe per slide. The slides were washed in a solution containing 0.2× SSC and 0.2% SDS for 5 min, incubated in 2× SSC for 2 min, treated with RNAse A (10 µg/ml) in 2× SSC for 20 min and equilibrated in TBS (0.1 M Tris–HCl pH 7.5, 0.4 M NaCl) for 5 min. Hybrids were detected using the Digoxigenin Nucleic Acid Detection kit according to the manufacturer's instructions (Roche). After signal visualization, the slides were dehydrated and mounted in Permount (Fisher Scientific). Photomicrographs were taken using a BX51 microscope (Olympus, Tokyo, Japan) with a bright-field condenser.

Modelling of the CoMir structure

Structural modelling was performed with a package Modeller, release 8v2 (Sali and Blundell 1993). For each sequence independent models were built based on five Kunitz STI structures obtained from the Protein Data Bank (PDB): 1AVA_C-BASI (1.9 Å) (Vallee et al. 1998),

1AVU-KTI3 (2.3 Å) (Song and Suh 1998), 1EYL-WCI (1.9 Å) (Ravichandran et al. 2001), 1R8N-DRTI (1.75 Å) (Krauchenco et al. 2003) and 1TIE-IDE3 (2.5 Å) (Onesti et al. 1991). For each alignment, 20 models were obtained and the model with the best Modeller objective function value was used for the structural analysis.

Protein expression and purification

The pGEMCoMirSS construct was digested with *Nco*I and *Bam*HI (Invitrogen) and the resulting DNA fragment inserted into a pET32a vector (Novagen, Madison, WI, USA), fused in frame downstream of Thiorredoxin (Trx) tag and 6× His-Tag, giving rise to the construct pET32aTrx::CoMirSS. This construct and pET32a were used to transform Origami B (DE3) cells. The transformed cells were grown in LB medium containing ampicillin (50 μg/ml) and kanamycin (15 μg/ml) under agitation (200 rpm) at 37°C overnight. A portion of the initial inoculum was diluted in LB (2 L) to an optical density (OD_{600}) of 0.1 and incubated under agitation at 37°C until it reached an OD_{600} of 0.8. The protein expression was induced by the addition of IPTG to a final concentration of 1.0 mM. The cells were incubated for 6 h at 28°C with shaking (200 rpm), harvested by centrifugation and subjected to a solubility test. The pellets were resuspended in a lysis buffer (10 μg/ml DNAseI, 20 mM Tris–HCl pH 7.4, 5% glycerol, 500 mM NaCl, 5 mM imidazole) and sonicated ten times for 15 s at 30% of maximum power in a Sonifier Sonics Vibra-cell. Insoluble debris were removed by centrifugation and the clear supernantants were submitted to Immobilized Metal Affinity Chromatography (IMAC), being loaded onto a 5 ml Ni^{2+} HisTrap FF crude column (GE Healthcare) using a AKTA-FPLC system. The proteins were eluted with a concentration gradient of imidazole (5–500 mM in 15 CV). After sample collection and analysis by SDS–PAGE, fractions containing partially purified proteins were combined and dialysed against 20 mM Tris–HCl pH 8.0, 20 mM NaCl and 5% glycerol overnight. For ion exchange chromatography, samples were loaded onto a 1-ml HiTrap Q HP column (GE Healthcare), using a AKTA-FPLC system. The proteins were eluted with a concentration gradient of NaCl (20–1,000 mM in 15 CV). The fractions collected were analysed by SDS–PAGE. Fractions containing purified Trx::CoMirSS and Trx were pooled and dialysed against 50 mM Tris HCl pH 8.0 overnight. The samples were then concentrated to 1 ml using an Amicon Ultra-15 Centrifugal Filter Unit 10 kDa membrane (Millipore, Billerica, MA, USA). Purified Trx::CoMirSS and Trx were quantified based on their absorbance at 280 nm, using a calculated extinction coefficient of 1.062 and 0.685 g L^{-1} cm^{-1}, respectively.

Proteolytic inhibition assays

The inhibitory activity of Trx::CoMirSS and Trx were determined by measuring the residual proteolytic activity. Before the anti-proteolytic assays, Trx::CoMirSS samples were heated at 60°C for 10 min and then incubated at room temperature for 20 min. Enzymes were pre-incubated/activated for 10 min in enzyme buffer solution containing increasing concentrations of the inhibitor protein tested. Afterwards, specific chromogenic substrates (see below) were added to those samples. The reactions were performed in a 96-well plate in a final volume of 250 μl, being accompanied for 10, 20 and 30 min. To block the reactions, 40 μl of 30% (v/v) acetic acid were added to the samples. Substrate hydrolysis was measured as the change in absorbance at 405 nm. Trypsin (20 μg/ml), subtilisin (1.3 μM) and chymotrypsin (1.6 μM) were activated by incubation for 10 min at 37°C in 50 mM Tris–HCl, pH 8.0, containing 0.02% $CaCl_2$. Human plasma kallikrein (HuPK—11 nM), human neutral elastase (HNE—0.2 μM) and porcine pancreatic elastase (PPE—0.2 μM) were activated for 10 min at 37°C in 50 mM Tris–HCl, pH 8.0, containing 0.5 M NaCl. The residual hydrolytic activity of the trypsin and HuPK were measured using Bz-Arg-pNan (BAPA—10 mM) and H-D-Pro-Phe-Arg-pNA (5 mM) as the chromogenic substrate, respectively. For the HNE and PPE assays, Suc-Ala-Ala-Pro-Val-pNA (11 mM) was used as the chromogenic substrate. Subtilisin and chymotrypsin activities were evaluated using the substrate Suc-Ala-Ala-Pro-Phe-pNA (4 mM). Ki values were determined by adjusting the experimental points to the equation for tight binding, using Morrison′s procedure with the GraFit program.

Nucleotide and protein sequence analysis

Sequencing was done in an ABI Prism 3700 sequencer (Applied Biosystems, Foster City, CA, USA) and database searches were performed using BLAST (Altschul et al. 1990). Protein prediction and analyses were done using PROSITE (http://ca.expasy.org/prosite), PFAM (http://pfam.sanger.ac.uk), PSIPRED (http://www.psipred.net/psiform.html) and PSORT (http://psort.hgc.jp). The proteinase inhibitor classification described was based on the MEROPS database (http://merops.sanger.ac.uk). Sequence alignment was carried out using CLUSTAL W 1.8 (Thompson et al. 1994) and edited using the GeneDoc platform (Nicholas and Nicholas 1997). The phylogenetic tree was inferred by using the program MEGA version 4.1 (Tamura et al. 2007). The tree was constructed as a consensus of 10,000 bootstrap replicates, using the Neighbour-Joining tree inference and JTT matrix for amino acid substitutions (Jones et al. 1992).

Results

Sequence analysis of CoMir

Coffee ESTs induced during leaf miner infestation were identified using nylon cDNA arrays containing clones from subtracted cDNA libraries (Mondego et al. 2005). One of these (SSH101B04) is similar to the tumour-related protein NF34 from tobacco (Karrer et al. 1998). The sequence from another EST (SSH104C02) that overlapped with the SSH101B04 clone was used to design primers for a 5′RACE amplification strategy. A single RACE product of 707 bp was cloned and sequenced. An open reading frame of 642 bp was detected, giving rise to a polypeptide of 214 amino acids (Fig. 1). This protein was significantly similar to the root-knot nematode-induced tomato gene *LeMir* (E-value 1e—36; 46% similarity; Brenner et al. 1998), to the taste-modifying protein miraculin (E-value 2e—31; 41% similarity; Theerasilp and Kurihara 1988) and to the tumour-related protein NF34 (E-value 2e—40; 48% similarity; Karrer et al. 1998). Since the full-length sequence was similar to both the *LeMir* and *miraculin* genes, it was named *CoMir* (*Co*ffee *Mir*aculin-like gene).

A Southern blot was carried out to verify whether *CoMir* was a member of a multigene family. *Eco*RI and *Eco*RV, restriction enzymes that do not have cut sites in *CoMir* cDNA sequence (Suppl. Fig. S1), were used in total DNA digestion reactions. The EST SSH104C02 (the 3′of *CoMir*) probe hybridized to several fragments on the Southern blot (Fig. 2). Four *Eco*RI fragments and four *Eco*RV fragments gave hybridization signals (Fig. 2), indicating the presence of at least four *CoMir*-like genes.

An alignment of MLPs (CoMir, miraculin, NF34, LeMir, PtdTI4, albumin, RlemMLP2) with the structurally resolved Kunitz STI (KTI3, BASI, WCI, DRTI, BASI) revealed that the MLPs have secondary structural idiosyncratic traits (Fig. 3a). The positively charged residues (Arg and Lys) are responsible for the trypsin inhibition of Kunitz STI (Laskowski and Kato 1980) being located between β-sheets A4 and B1. In CoMir, the only positively charged residue found in this loop was an Arg in position 92 (Fig. 3, asterisk). With the exception of CoMir, the MLPs contain two additional Cys near the C-terminal end in a loop region between the β-sheets C1 and C2 (Fig. 3a, box IV). In CoMir, only one of these Cys

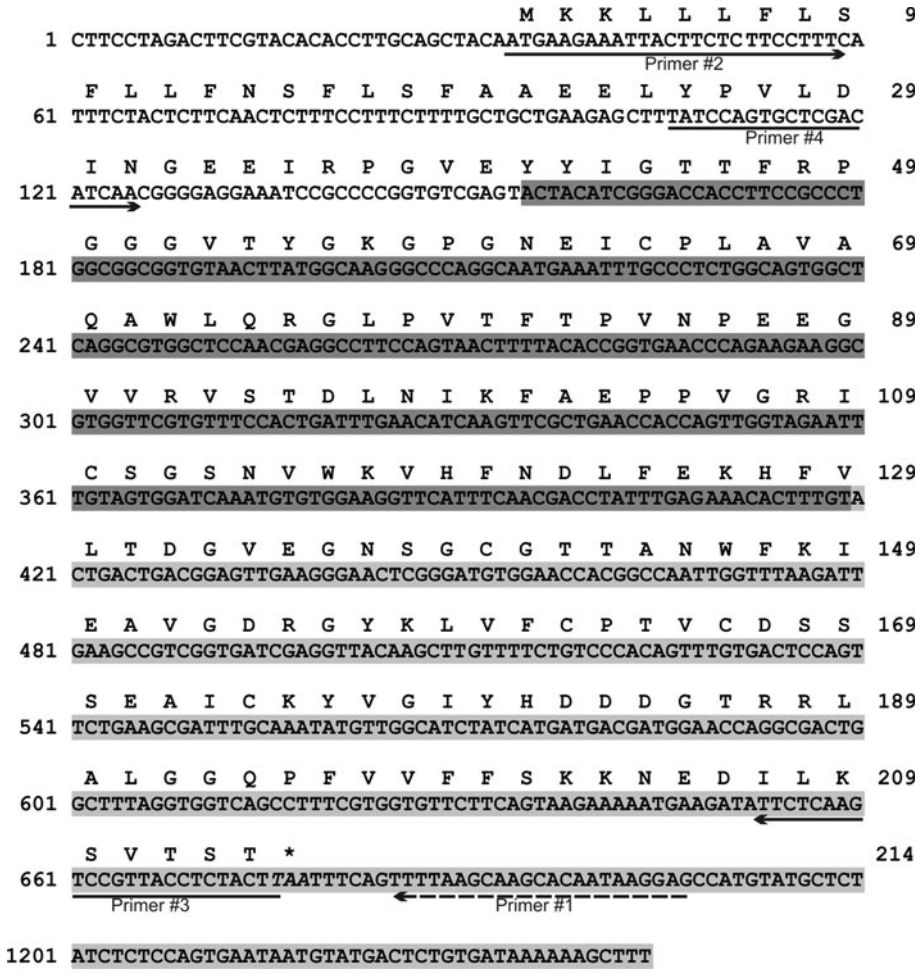

Fig. 1 *CoMir* nucleotide and amino acid sequences. The amino acid sequence is on the *top lines* and the nucleotide sequence is shown below. *Dark grey* background, sequence of EST SSH102B04. *Light grey* background, sequence of EST SSH104C02. *Asterisk* stop codon. The primer sites used for RT-PCR (primers #2, 3 and 4) are indicated by *arrows*. *Dashed arrows* indicate the primer #1 site used in 5′ RACE-PCR, giving rise to a 707-bp PCR product. *Numbers* on the *left* refer to the DNA sequence. *Numbers* on the *right* refer to the protein sequence

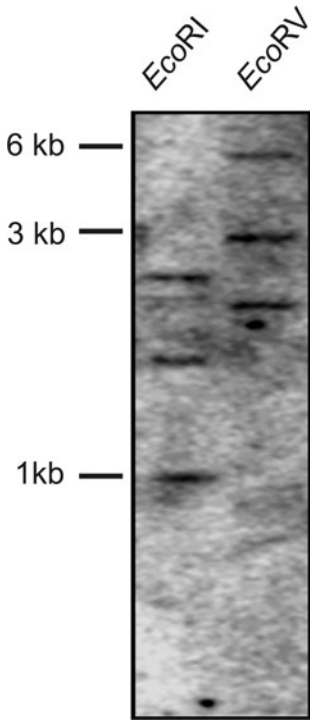

Fig. 2 *CoMir* Southern-blot analysis. Genomic DNA of resistant plants from a hybrid progeny H14954-29 (derived from crosses between *C. arabica* and *C. racemosa*) was digested with *Eco*RI and *Eco*RV, applied in an agarose gel, blotted onto a nylon membrane and hybridized with [α-32P]dCTP-labelled EST SSH104C02 (3′ *CoMir*) as a probe. DNA sizes expressed in kb are shown on the *left*. The same hybridization pattern was observed in coffee leaf miner susceptible plants from the progeny H14954-29 (data not shown)

(Cys166) is located at this loop. The other Cys (Cys140) are present in a Gly-rich loop between *β*-sheets B3 and B4 (Fig. 3a, box III).

To verify whether Cys140 and Cys166 form a third disulfide bond in CoMir, this protein was modelled based on five Kunitz STI protein structures available in the PDB. Figure 4a represents the model of CoMir based on the DRTI structure (1R8N). The LeMir and miraculin proteins were also modelled, confirming that the closeness of the sulphur atoms of the two additional Cys located in the loop between sheets C1 and C2 (Cys151-Cys154) form a third disulphide bridge, as mentioned by Paladino et al. (2008). The distance between Cys166 and Cys140 varied significantly in each model built (Suppl. Fig. S2). For the model based on the structure of 1AVU (KTI3), the distance between the sulphur atoms was 26.1 Å, but in the model based on the DRTI (18RN) structure the sulphur atoms were approximately 12.6 Å apart (Suppl. Table S1). The alignment of the five proteins with CoMir and the other MLPs was analysed, observing that in the loop containing Cys140 there was a variation in the length of the gaps for each of the sequences (Fig. 3a, box III). The length of these gaps was correlated with the distances between the sulphur atoms of the two Cys (Suppl. Table S1). When CoMir was superimposed with the structure of IDE3 (1TIE), two prominent loops were observed (Fig. 4b). The first was the region between sheets C1 and C2, named as the Cys rich-loop, and the second was a loop between sheets B3 and B4, which contained sequence similarity with the P-loop motifs of nucleoside-binding proteins such as the Gly-rich loops of PR-10 proteins (Fig. 4c).

The alignment of the Kunitz STI proteins (Fig. 3a) was used to construct a phylogenetic tree (Fig. 3b), which indicated that CoMir clustered together with other MLPs, such as LeMir, NF34 and miraculin.

CoMir expression pattern

To evaluate the *CoMir* expression profile during *L. coffeella* infestation, *CoMir* cDNA was used as a probe in blots containing RNA from coffee leaf miner infestation experiments. *CoMir* was up-regulated in resistant plants after oviposition (Ro) and its expression decreased after egg hatching and leaf miner death (Re). In susceptible plants, *CoMir* was slightly induced after oviposition (So) and no transcripts were detected after larval eclosion (Se), indicating that *CoMir* was repressed during herbivory in susceptible plants (Fig. 5a). Since treatment with the phytohormones MeJA, ABA and wounding treatments were reported as inducers of the PIs expression (Tsukuda et al. 2006; Huang et al. 2007), their influences on the expression of *CoMir* were examined. When applied to coffee plants, ABA (100 μM) resulted in the induction of *CoMir* 12 h after spraying (Fig. 5b). Figure 5c shows the induction of *CoMir* expression 12 h after wounding, decreasing after 24 h. The results of the MeJA challenge were inconsistent because there was a variation in the *CoMir* expression of the replicates (data not shown).

To determine the *CoMir* organ specificity, the *CoMir* cDNA probe was hybridized to RNA blots containing RNA from different coffee plant organs (Fig. 6). The *CoMir* expression was highest in green flower buds and decreased during later flower development (Fig. 6a). *CoMir* was highly expressed in early green fruits, being repressed throughout fruit maturation (Fig. 6b). In addition, *CoMir* transcripts were detected in the leaves and not detected in the coffee roots (Fig. 6a).

In situ hybridization was used to localize *CoMir* tissue-specific transcript accumulation (Fig. 7). Using antisense probes, *CoMir* transcripts were found in the xylem vessels of leaves, most specifically in wide vessels of the metaxylem (Fig. 7a–c). In flower buds, *CoMir* was expressed inside metaxylem vessels of the petals (Fig. 7e. g), in the vascular bundles, endothecium, tapetum and stomium of the anthers (Fig. 7h) and in the stigma xylem (Fig. 7j).

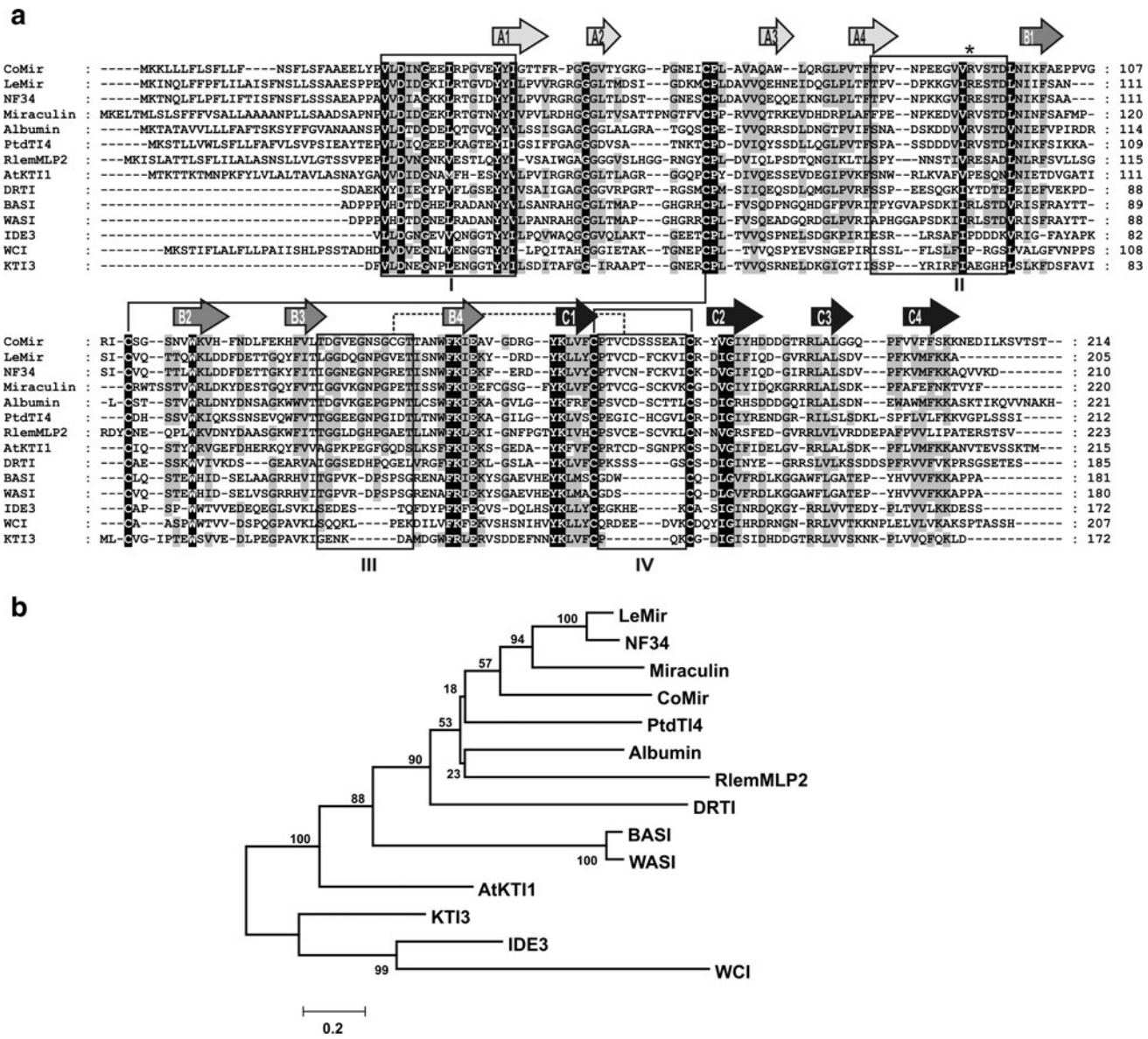

Fig. 3 CoMir sequence and phylogenetical analysis. **a** Alignment of CoMir with miraculin-like proteins and structurally resolved Kunitz STI proteins. *Black* background, 100% of conservation between amino acids. *Grey* background, conservation between amino acids of at least 60%. *SP* signal peptide. *Box I* N-terminal signature sequence of the Kunitz STI family: [(L/I/V/M)-X-D-X-(E/D/N/T/Y)-(D/G)-(R/K/H/D/E/N/Q)-X-(L/I/V/M)-X-(5)-Y-X-(L/I/V/M)]. *Box II* proteinase inhibitory reactive loop. *Box III* putative Gly-rich loop. *Box IV* Cys-rich loop specific for miraculin-like proteins. Kunitz STI conserved disulphide bridges are indicated by continuous *brackets*. The hypothetical third disulphide bond of CoMir is indicated by a *dashed bracket*. *Arrows* indicate putative CoMir β-sheets, whose nomenclature is based on McLachlan (1979). The accession numbers of the proteins are the following: CoMir (DQ993351), LeMir (T07871), NF34 (T03803), Miraculin (P13087), PtdTI4 (AAQ84217), Albumin (1802409A), RlemMLP2 (BAE79511), DRTI (AAY84867), KTI3 (P01070), AtKTI1 (NP_565061) WCI (AAC60537), IDE3 (P09943), BASI (P07596), WASI (P16347). The alignment was constructed with Clustal W 1.8 and edited with Gene Doc. **b** Unrooted phylogenetic tree of Kunitz STI proteins. The tree was constructed as a consensus of 100,000 bootstrap replicates, using Neighbour-Joining and JTT matrix parameters

Using the *CoMir* sense probe, no signal was detected in those tissues (Fig. 7d, f, i, k). Unfortunately, coffee fruits were recalcitrant to in situ fixation, which hindered the characterization of the tissue-specific expression of *CoMir* during coffee fruit/seed maturation (data not shown).

CoMir subcellular localization

To verify the subcellular localization of CoMir, a plasmid containing a *CoMir::mGFP* fusion was transiently expressed in onion epidermal cells using particle bombardment.

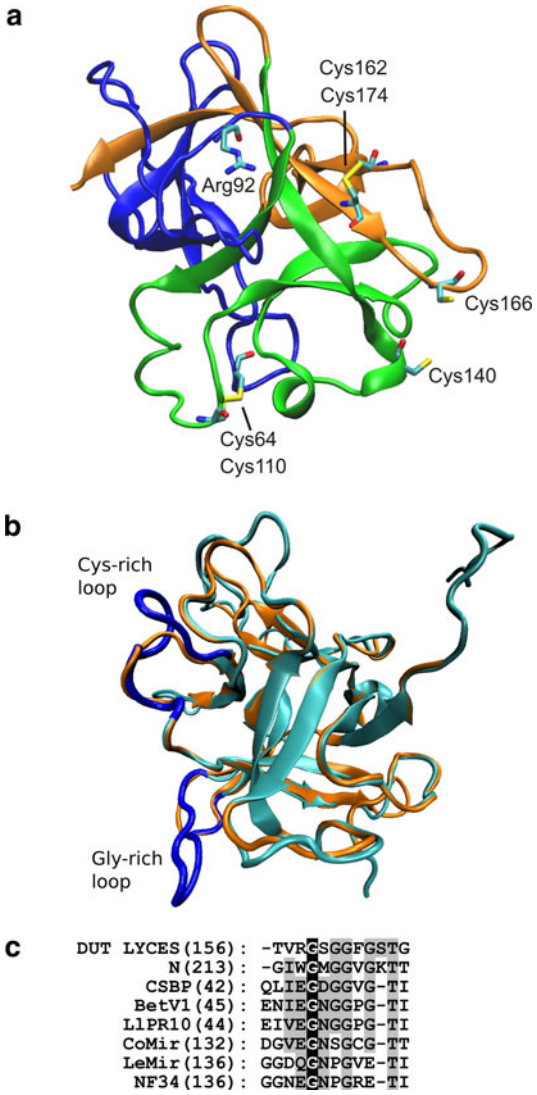

Fig. 4 3D molecular model of CoMir. **a** CoMir structure based on the DRTI protein (18RN). The fold preserves the 12 β-sheet structure of the Kunitz STI proteins. The sheets are classified into three groups according to MacLahlan (1979). *Blue sheets* A1 to A4, *green sheets* B1 to B4, and *orange sheets* C1 to C4. Cysteines and arginine in the reactive loop are indicated by *sticks* and *coloured* according to atom type. **b** Superimposition of the SD molecular model of CoMir (*light blue*) and IDE3 (*orange*). CoMir Cys-rich loop and Gly-rich loop are *coloured* in *dark blue*. **c** Protein sequence alignment of Gly-rich loops. The accession numbers are the following: DUTP_LYCES, *Lycopersicon esculentum* Deoxyuridine 5′-triphosphate nucleotidohydrolase (P32518); N, tobacco mosaic resistance gene (AAA50763); CSBP, *Vigna radiata* cytokinin-specific binding protein (BAA74451); BetV1, *Betula pendula* Major pollen allergen Bet v 1-A (P15494); LlPR10, *yellow* lupine pathogenesis-related protein Llpr10.1a (1XDF_A); CoMir (DQ993351); LeMir, (T07871); NF34 (T03803). Sequences were aligned with Clustal W 1.8 and edited with Gene Doc

The onion epidermis was treated with a sucrose solution to induce cell plasmolysis. Using this technique, CoMir was localized in the cytosol (Fig. 8a).

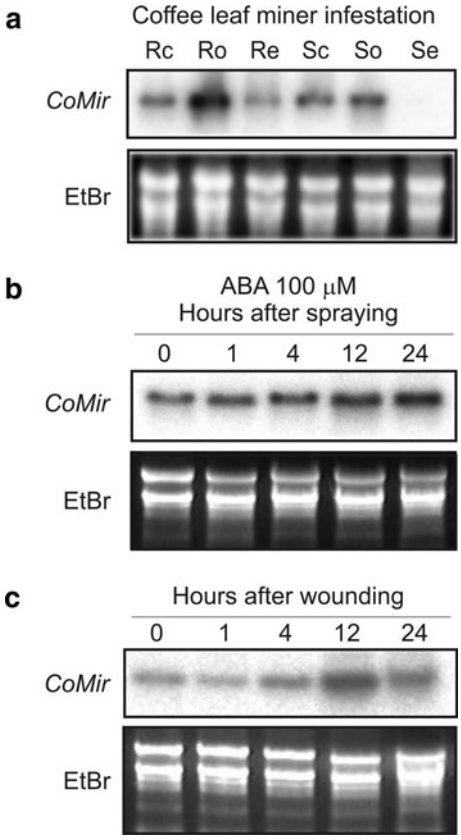

Fig. 5 *CoMir* expression profile during coffee leaf miner infestation, abscisic acid (ABA) and wounding treatments. Total RNA was extracted, separated electrophoretically in formaldehyde-agarose gels, blotted onto nylon membranes and hybridized with [α-32P]dCTP-labelled *CoMir* probe. **a** Leaves were infested as described previously (Mondego et al. 2005). *Rc* resistant plants not infested; *Ro* resistant plants after oviposition; *Re* resistant plants after larvae eclosion; *Sc* susceptible plants not infested; *So* susceptible plants after oviposition; *Se* susceptible plants after larvae eclosion. **b** Coffee plants were sprayed with a 100 µM ABA solution (dissolved in warm water) and incubated at 26°C for up to 24 h in constant light. *Numbers* at the *top* of the blot indicate time (h) after treatment. **c** The first pair of coffee plants leaves were wounded according to the method described by Reymond et al. (2000). Plants were incubated at 26°C for up to 24 h in constant light. *Numbers* at the *top* of the blot indicate time (h) after treatment. Replicates of these experiments resulted in the same expression profiles. Ethidium bromide stained rRNA (EtBr) was visualized for RNA loading

Protein expression and proteolytic inhibitory activity of CoMir

The CoMir protein with no signal peptide (*CoMir*SS) was overexpressed in *E. coli*. The strain Origami B (DE3) was transformed by the construct pET32a-Trx::CoMirSS containing a 6× His-Tag (indicated for IMAC purification) and Trx tag, which enhances the solubility of the fusion protein. Origami B (DE3) contains *trxB* and *gor* mutations, which increase disulphide bond formation in the *E. coli*

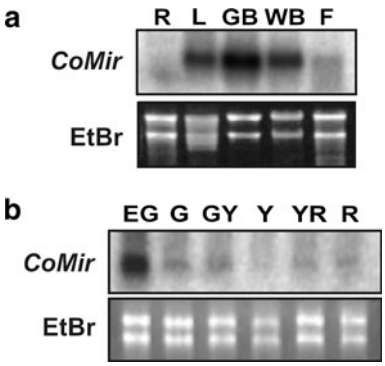

Fig. 6 *CoMir* expression profile in different organs of coffee plants. Total RNA was extracted, separated electrophoretically in formaldehyde-agarose gels, blotted onto nylon membranes and hybridized with [α-32P]dCTP-labelled *CoMir* probe. **a** RNA blot containing RNA from roots (R), leaves (L), green flower buds (GB), white flower buds (WB) and open flowers (F). **b** RNA blot containing RNA from different stages of coffee fruit development: *Early green* (EG), *Green* (G), *Green-Yellow* (GY), *Yellow* (Y), *Yellow-Red* (YR) and *Red* (R). Ethidium bromide stained rRNA (EtBr) was visualized for RNA loading

cytoplasm. The same procedure was performed with an empty pET32a plasmid to produce Trx protein as a control. After overexpression and bacterial lysis, Coomassie Blue stained SDS–PAGE showed an induced Trx::CoMirSS fusion protein in the soluble fractions with a molecular mass of approximately 40 kDa (Fig. 9a, left panel). Concerning Trx, we have found an induced protein of approximately 20 kDa (Fig. 9b, left panel). The fusion proteins were purified by IMAC and ion exchange chromatography (Fig. 9a and b, right panel). To avoid possible contaminating proteinases during the Trx::CoMirSS purification, which could interfere in the anti-proteolytic assays, the fusion protein sample was incubated at 60°C for 10 min and then tested for proteinase inhibitory activity. The serine proteinases trypsin, subtilisin, chymotrypsin, HNE, HuPK and PPE and chromogenic substrates recommended for each enzyme (see Material and methods) were used in the reactions. Approximately 50% of trypsin activity was inhibited by the addition of 100 μg of Trx::CoMirSS, with an inhibition constant (Ki) of 12.5×10^{-7} M (Fig. 9c). Trx::CoMirSS did not inhibit any of the other proteinases tested (data not shown). Trx did not inhibit trypsin (Fig. 9c) or any other proteinase (data not shown).

Discussion

CoMir is a Kunitz STI miraculin-like protein with interesting structural characteristics

Database searches revealed that *CoMir* is similar to miraculin-like proteins (MLPs) such as LeMir from tomato (Brenner et al. 1998), miraculin from *R. dulcifica* (Theerasilp and Kurihara 1988) and the tumour-related protein NF34 from tobacco (Karrer et al. 1998); all of which belong to the Kunitz STI family of PIs. MLPs have been associated with biotic stress (Karrer et al. 1998; Brenner et al. 1998; Tsukuda et al. 2006). The isolation of a MLP gene in a subtracted cDNA library, enriched with genes preferentially induced during coffee leaf miner infestation, stimulated the evaluation of the expression profile and structural characteristics of CoMir. The Southern blot results indicated that *CoMir* was a member of a multigene family (Fig. 2). This is quite common in proteinase inhibitors, even more so in an allopolyploidy species such as *C. arabica*. Further experiments are needed to isolate the other *C. arabica* MLPs and to dissect their mechanisms of gene expression control.

The alignment of the MLPs with other Kunitz STI demonstrated that the members of this family varied with respect to their Cys content, which is more prominent in a loop region near the C-terminal end. The modelling analysis used corroborated with the data of Paladino et al. (2008), showing that the closeness of these Cys residues near the C-terminal end could form a third disulphide bridge in the MLPs. Recently, the first crystal structure from this group of proteins was released (PDB, 3IIR), showing the presence of a third disulfide bridge in a loop near the C-terminal end (Gahloth et al. 2010). However, CoMir only contains one Cys in this region (position 166). CoMir models based on DRTI (18RN) and BASI (1AVA_C) structures indicated that Cys166 could form a third disulphide bridge, with Cys140 located in a Gly-rich loop. The great variability of the distances between the sulphur atoms of Cys140 and Cys166 was surprisingly correlated with the different lengths of the gaps of the Kunitz STI in the region aligned with the Gly-rich loop between the β-sheets B3 and B4 (Figs. 3a, box III, 4c) present in the MLPs. The longer the gap, the less probable was the formation of the third disulphide bridge (Suppl. Table S1). However, one cannot discard the possibility that these Cys residues could form intermolecular disulfide bridges with another CoMir monomer. The positioning of these Cys residues in the models based on 18RN (DRTI) and 1AVA_C (BASI), the high conformational flexibility of the loops containing Cys140 and Cys166, and the resolved structure of a MLP containing three disulfide bridges (Gahloth et al. 2010) provide a structural basis for the possibility of the formation of a third disulphide bridge in CoMir. The aforementioned Gly-rich loop present in CoMir resembled the P-loop motif found in many nucleotide- and phosphate-binding proteins (Saraste et al. 1990), including the pathogenesis-related protein PR-10 (Koistinen et al. 2005). More analyses (i.e., nucleotide binding assays) are needed to elucidate whether this loop has a functional role.

The N-terminus of the MLPs contains a signal peptide for secretion to the apoplast (Brenner et al. 1998; Tsukuda

Fig. 7 In-situ localization of *CoMir* mRNA. Transversal sections (10 μM) of coffee tissues were hybridized with *CoMir* antisense (**a**, **b**, **c**, **e**, **g**, **h**, **j**) and sense (**d**, **f**, **i**, **k**) RNA probes (see "Materials and methods"). Hybridization corresponds to a *blue* signal in the tissue. Leaves (**a**, **b**, **c**, **d**), *white* flower bud petal (**e**, **f**, **g**), anther (**h**, **i**) and stigma (**j**, **k**). *Mx* metaxylem; *Px* protoxylem; *VB* vascular bundles; *St* stomium; *Tp* tapetum; *Et* endothecium. Bars = 30 μM. Experiments were done in triplicate resulting in the same expression pattern

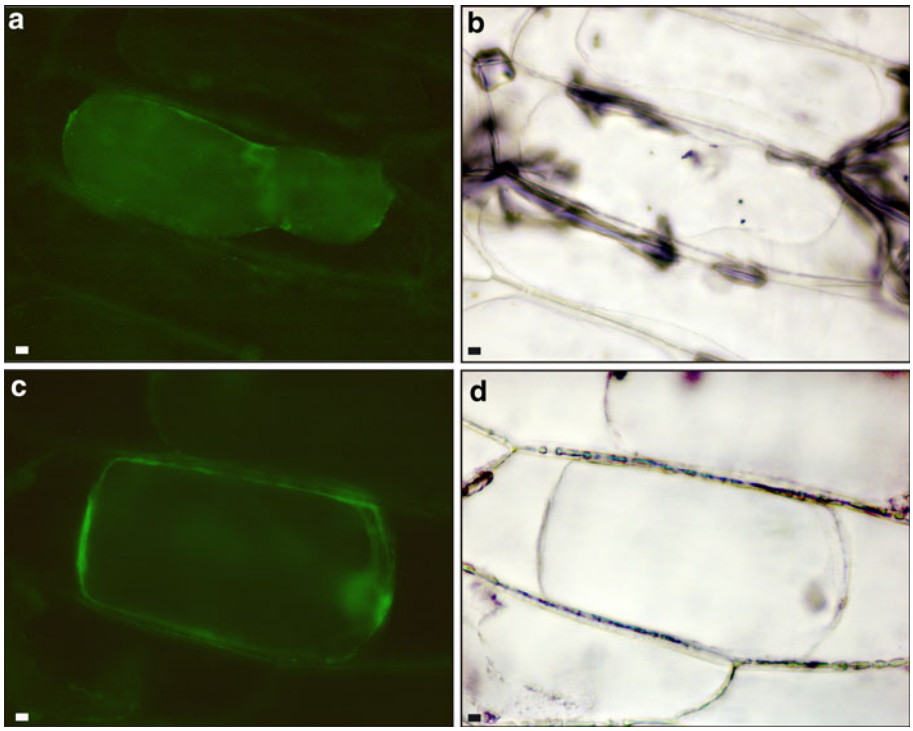

Fig. 8 Subcellular localization of CoMir. Onion epidermis cells were bombarded with plasmids containing GFP fusions. *Left* CoMir::mGFP5 expression (**a**) and mGFP5 expression (**c**) in *dark field* fluorescence. *Right Bright field* images of CoMir::mGFP5 (**b**) and mGFP5 (**d**). *Bars* 10 μM. Experiments were done in triplicate resulting in the same fluorescence pattern

et al. 2006). Hirai et al. (2010) showed that *R. dulcifica* miraculin::GFP fusion protein was secreted and accumulated in the intercellular spaces of tomato hypocotyls. However, the transient expression of the CoMir::GFP fusion protein demonstrated that CoMir was located in the cytosol (Fig. 8a). Although one cannot rule out the fact that the CoMir::GFP targeting of the cytoplasm may be due to uncorrected folding or uncorrected signal peptide proteolysis of the protein fusion, this fluorescence pattern was similar to that found by Tsukuda et al. (2006), who analysed rough lemon MLPs. The cytosolic localization of the MLPs suggests that their putative role against biotic stress does not need an extracellular location or, alternatively, that they may have other intracellular functions.

Regarding CoMir antiproteolytic activity, even though the anti-enzymatic activity of Trx::CoMirSS against trypsin is quite weak when compared with other Kunitz STI, Trx alone does not have activity against this proteinase (Fig. 9). The fact that trypsin is not inhibited by Trx indicates that CoMir indeed inhibits trypsin.

Implications of *CoMir* expression in plant development and stress response

Our results demonstrated that *CoMir* was preferentially expressed in the early stages of flower and fruit development (Fig. 6a, b). This expression pattern is in agreement with previous reports showing that PIs are expressed in immature tissues (Shatters et al. 2004). On the other hand, proteinases were found to be up-regulated during fruit maturation and flower senescence (Xu and Chye 1999; Wagstaff et al. 2002). These results indicate that proteolytic activity during plant development is regulated by PI expression. Even though the *CoMir* expression declined in mature fruits, this PI may be stored in the fruit during later stages, acting as a seed storage protein.

In situ hybridization showed that *CoMir* is expressed in the anther endothecium, tapetum and stomium in white flower buds (Fig. 7h). These three tissues suffer programmed cell death (PCD), which is essential for microspore maturation and release (Wu and Cheun 2000). De Guzman and Riggs (2000) demonstrated that proteolysis increases during anther development and is temporally correlated with the PCD of anther tissues, preceding pollen liberation. Together with the RNA blot results, which showed that *CoMir* is down-regulated in senescent open flowers (Fig. 6a), in situ results suggested that CoMir may be a proteolytic inhibitor during early microsporogenesis, whose expression is repressed throughout anther development.

The expression of *CoMir* in the metaxylem cells of leaves (Fig. 7a–c), petals (Fig. 7e, g) and stigma (Fig. 7j) was shown. Another Kunitz STI (CaTPI-1) is expressed in xylem vessels (Jiménez et al. 2007), and this protein was localized in the cell wall of the protoxylem but its transcription site was not assessed. After deposition of secondary cell wall thickenings, the xylem vessels suffer autolysis by PCD (Kozela and Regan 2003), which is preceded by serine and cysteine proteinase expressions (Groover and Jones 1999; Demura et al. 2002). Groover and Jones (1999) found that a STI applied exogenously to a *Zinnia elegans* cell

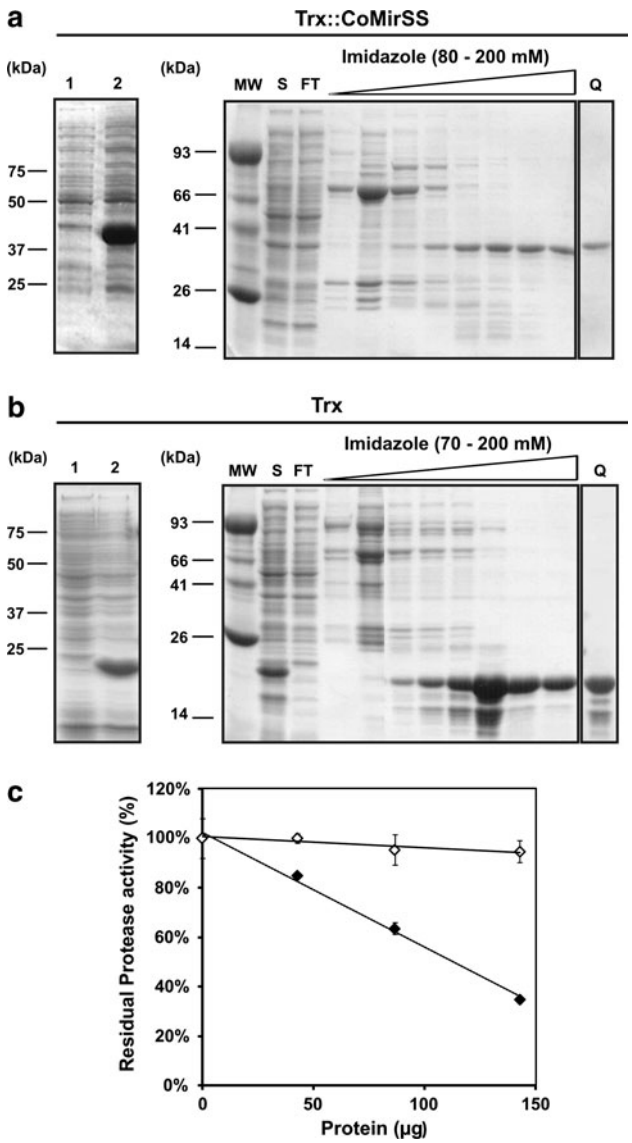

Fig. 9 Production of recombinant Trx::CoMirSS and in vitro assay of trypsin inhibitory activity. Expression and purification of Trx:CoMirSS (**a**) and Trx (**b**). *Left panel* SDS–polyacrylamide (12% w/v) gel analysis of soluble fractions of non-induced cells (*lane 1*) and cells induced with 1.0 mM IPTG (*lane 2*). *Right panel* SDS–polyacrylamide (12% w/v) gel analysis of IMAC purification. *Lane MW* molecular marker (LNBio); *Lane S* soluble fraction of cells extract applied in IMAC resin; *Lane FT* Flow-Through of purification; increasing concentrations of imidazole in buffer A were applied to the column, resulting in the remaining samples applied in the gel; *Lane Q* purified proteins after ion exchange chromatography. **c** Dose-responses of Trx::CoMirSS (*Filled diamond*) and Trx (*Open diamond*) on proteinase inhibitor activities. Increasing concentrations of proteins were tested for their trypsin inhibitor activities, which were spectrophotometrically measured using BAPA as the chromogenic substrate. A relative percentage of trypsin (0.6 µg/reaction) activity without addition of inhibitors was obtained. Values indicate the mean of the replicate samples (±SD)

culture, blocked tracheal element (TEs) differentiation and cell death, suggesting that an endogenous PI negatively regulates TEs cell death. The evidence of Kunitz STI gene expression and protein localization in the xylem vessels reinforces the potential role of PIs in preventing proteolysis during TE differentiation. The fact that *CoMir* is preferentially expressed in young tissues and, probably, just before the secondary cell wall formation of the xylem, suggests that this coffee MLP may act as a regulator of proteolysis during xylogenesis.

The accumulation of *CoMir* mRNA in response to wounding was similar to that found for various genes encoding PIs (Ryan 1990). ABA also induced the expression of *CoMir* (Fig. 5b). Plants with reduced ABA levels were found to be more susceptible to insect feeding (Thaler and Bostock 2004; Bodenhausen and Reymond 2007), indicating that this phytohormone is implicated in plant defence against insects. Therefore, *CoMir* induction by such treatments (wounding and ABA) may be associated with insect resistance. Several studies on serine PIs revealed their potential as inhibitors of lepidopteran serine proteinases, affecting insect digestion and retarding larval development (Pompermayer et al. 2001; Rodrigues-Macedo et al. 2003; Liu et al. 2004; Sumikawa et al. 2010). However, *CoMir* expression was repressed in the susceptible genotype during coffee leaf miner herbivory (Fig. 5a). The down-regulation of a PI during a plant-herbivore interaction is intriguing and suggests that *L. coffeella* larvae may manipulate the coffee plant defence system for their own benefit. This phenomenon was documented in plant–caterpillar interactions where chemical compounds present in the insect saliva counteracted the production of plant defence secondary metabolites (Musser et al. 2002; Bede et al. 2006) and proteinase inhibitors (Lawrence et al. 2007).

Previous reports showed that insect oviposition fluids activate plant defence (Doss et al. 2000; Hilker et al. 2005; Little et al. 2007). Furthermore, Little et al. (2007) detected the up-regulation of two serine PIs after *Pierid* butterfly oviposition in *A. thaliana* leaves. A similar expression profile (CoMir induction after oviposition) was observed in our data (Fig. 5a). It is possible that the amount of CoMir prior to egg hatching in resistant plants would inhibit *L. coffeella* caterpillar eclosion or its growth inside leaf mines by blocking the digestive proteinases of the neonate caterpillar. Given that coffee leaf miner does not accept artificial diets (Guerreiro-Filho et al. 1998), one possibility to evaluate whether CoMir actually deters *L. coffeella* development would be to infiltrate coffee leaves with CoMirSS, similar to the experiment performed with Bt endotoxin (Guerreiro-Filho et al. 1998). However, recombinant CoMirSS is not stable in water or in any other non-oxidative buffer (data not shown), making it difficult for such a protein to be active under the natural physiological conditions during approximately 10 days (completion period of the *L. coffella* life cycle).

It is noteworthy that previous studies have reported that after insect oviposition, plants can avoid egg development by producing punctiform necrotic lesions surrounding the egg deposition sites, resembling a HR (Shapiro and Devay 1987; Balbyshev and Lorenzen 1997; Little et al. 2007). A similar phenotype was detected at the oviposition site of *L. coffeella* larvae in highly resistant coffee plants (Medina-Filho et al. 1977; Guerreiro-Filho et al. 1991; Mondego et al. 2005). The MLP tumour-related protein NF34 elicited HR in the tobacco mosaic virus (TMV)-susceptible tobacco plants, when over-expressed by a TMV expression vector (Karrer et al. 1998), and an Arabidopsis Kunitz trypsin inhibitor (AtKTI1) that is similar to the MLPs was shown to be a modulator of plant pathogen-related PCD (Li et al. 2008). These data raise the possibility that CoMir acts in a HR-like defence mechanism against *L. coffeella*. The production of transgenic coffee plants over-expressing or under-expressing *CoMir* would be a further step in an attempt to unravel the function of this gene.

Acknowledgments The authors are grateful to Daniel Ramiro and Silvia Mathiessen (IAC) for rearing the insects, Dr. Nilson Ivo Zanchin (Laboratório Nacional de Luz Sincrotron) and Prof. Dr. Fabio Maranhão Costa (Departamento de Genética, Evolução e Bioagentes, IB, UNICAMP) for the use of the fluorescence microscopes, and Edna Santos (Departamento de Genética, Evolução e Bioagentes, IB, UNICAMP) and Sebastião Militão (Departamento de Biologia Vegetal, IB, UNICAMP) for technical assistance. J.M.C.M. and M.P.D. were recipients of fellowships from FAPESP (Fundação de Amparo a Pesquisa do Estado de São Paulo). L.M. received a PBIG-UNICAMP fellowship. S.C.R. received a fellowship from CAPES (Conselho de Aperfeiçoamento de Pesquisa em Ensino Superior). M.M. received a research fellowship from CNPq (Conselho Nacional de Desenvolvimento Científico e Tecnológico). This research was supported by the Consórcio Brasileiro de Pesquisa e Desenvolvimento do Café, FAEPEX/UNICAMP (project—040504), FAPESP (project—03/09361-4) and CNPq (479800/2004-9).

References

Altschul SF, Gish W, Miller W, Myers EW, Lipman DJ (1990) Basic local alignment search tool. J Mol Biol 215:403–410

Balbyshev NF, Lorenzen JH (1997) Hypersensitivity and egg drop: a novel mechanism of host plant resistance to Colorado potato beetle (Coleoptera: Chrysomelidae). J Econ Entomol 90:652–657

Bede JC, Musser RO, Felton GW, Korth KL (2006) Caterpillar herbivory and salivary enzymes decrease transcript levels of *Medicago truncatula* genes encoding early enzymes in terpenoid biosynthesis. Plant Mol Biol 60:519–531

Bodenhausen N, Reymond P (2007) Signaling pathways controlling induced resistance to insect herbivores in *Arabidopsis*. Mol Plant Microbe Interact 20:1406–1420

Brenner ED, Lambert KN, Kaloshian I, Williamson VM (1998) Characterization of *LeMir*, a root-knot nematode-induced gene in tomato with an encoded product secreted from the root. Plant Physiol 118:237–247

De Guzman R, Riggs CD (2000) A survey of proteinases active during meiotic development. Planta 210:921–924

Demura T, Tashiro G, Horiguchi G, Kishimoto N, Kubo M, Matsuoka N, Minami A, Nagata-Hiwatashi M, Nakamura K, Okamura Y, Sassa N, Suzuki S, Yazaki J, Kikuchi S, Fukuda H (2002) Visualization by comprehensive microarray analysis of gene expression programs during transdifferentiation of mesophyll cells into xylem cells. Proc Natl Acad Sci USA 99:15794–15799

Doss RP, Oliver JE, Proebsting WM, Potter SW, Kuy S, Clement SL, Williamson RT, Carney JR, DeVilbiss ED (2000) Bruchins: insect-derived plant regulators that stimulate neoplasm formation. Proc Natl Acad Sci USA 97:6218–6223

Gahloth D, Selvakumar P, Shee C, Kumar P, Sharma AK (2010) Cloning, sequence analysis and crystal structure determination of a miraculin-like protein from *Murraya koenigii*. Arch Biochem Biophys 494:15–22

Groover A, Jones AM (1999) Tracheary element differentiation uses a novel mechanism coordinating programmed cell death and secondary cell wall synthesis. Plant Physiol 119:375–384

Guerreiro-Filho O, Medina-Filho HP, Carvalho A (1991) Fontes de resistência ao bicho-mineiro, *Perileucoptera coffeella*, em *Coffea* spp. Bragantia 50:45–55

Guerreiro-Filho O, Denolf P, Peferoen M, Decazy B, Eskes AB, Frutos R (1998) Susceptibility of the coffee leaf miner (*Perileucoptera* spp.) to *Bacillus thuringiensis* delta-endotoxins: a model for transgenic perennial crops resistant to endocarpic insects. Curr Microbiol 36:175–179

Guerreiro-Filho O, Silvarolla MB, Eskes AB (1999) Expression and mode of inheritance in coffee to leaf miner *Perileucoptera coffeella*. Euphytica 105:7–15

Hansen D, Macedo-Ribeiro S, Veríssimo P, Yoo Im S, Sampaio MU, Oliva ML (2007) Crystal structure of a novel cysteinless plant Kunitz-type protease inhibitor. Biochem Biophys Res Commun 360:735–740

Haseloff J (1999) GFP variants for multispectral imaging of living cells. Methods Cell Biol 58:139–151

Hilker M, Stein C, Schroder R, Varama M, Mumm R (2005) Insect egg deposition induces defense responses in *Pinus sylvestris*: characterisation of the elicitor. J Exp Biol 208:1849–1854

Hirai T, Sato M, Toyooka K, Sun HJ, Yano M, Ezura H (2010) Miraculin, a taste-modifying protein is secreted into intercellular spaces in plant cells. J Plant Physiol 167:209–215

Huang Y, Xiao B, Xiong L (2007) Characterization of a stress responsive proteinase inhibitor gene with positive effect in improving drought resistance in rice. Planta 226:73–85

Jiménez T, Martín I, Labrador E, Dopico B (2007) A chickpea Kunitz trypsin inhibitor is located in cell wall of elongating seedling organs and vascular tissue. Planta 226:45–55

Jones BL, Fontanini D (2003) Trypsin/alpha-amylase inhibitors inactivate the endogenous barley/malt serine endoproteinase SEP-1. J Agric Food Chem 51:5803–5814

Jones DT, Taylor WR, Thornton JM (1992) The rapid generation of mutation data matrices from protein sequences. Comput Appl Biosci 8:275–282

Karrer EE, Beachy RN, Holt CA (1998) Cloning of tobacco genes that elicit the hypersensitive response. Plant Mol Biol 36:681–690

Koistinen KM, Soininen P, Venalainen TA, Hayrinen J, Laatikainen R, Perakyla M, Tervahauta AI, Karenlampi SO (2005) Birch PR-10c interacts with several biologically important ligands. Phytochemistry 66:2524–2533

Kozela C, Regan S (2003) How plants make tubes. Trends Plant Sci 8:159–164

Krauchenco S, Pando SC, Marangoni S, Polikarpov I (2003) Crystal structure of the Kunitz (STI)-type inhibitor from *Delonix regia* seeds. Biochem Biophys Res Commun 312:1303–1308

Laskowski M Jr, Kato I (1980) Protein inhibitors of proteinases. Annu Rev Biochem 49:593–626

Lawrence SD, Novak NG, Blackburn MB (2007) Inhibition of proteinase inhibitor transcripts by *Leptinotarsa decemlineata* regurgitant in *Solanum lycopersicum*. J Chem Ecol 33:1041–1048

Li J, Brader G, Palva ET (2008) Kunitz trypsin inhibitor: an antagonist of cell death triggered by phytopathogens and fumonisin b1 in *Arabidopsis*. Mol Plant 1:482–495

Little D, Gouhier-Darimont C, Bruessow F, Reymond P (2007) Oviposition by pierid butterflies triggers defense responses in *Arabidopsis*. Plant Physiol 143:784–800

Liu Y, Salzman RA, Pankiw T, Zhu-Salzman K (2004) Transcriptional regulation in southern corn rootworm larvae challenged by soyacystatin N. Insect Biochem Mol Biol 34:1069–1077

McLachlan AD (1979) Threefold structural pattern in the soybean trypsin inhibitor (Kunitz). J Mol Biol 133:557–563

Medina-Filho HP, Carvalho AP, Mônaco LC (1977) Melhoramento do cafeeiro. XXXVII—observações sobre a resistência do cafeeiro ao bicho mineiro. Bragantia 36:131–137

Mondego JMC, Guerreiro-Filho O, Bengtson MH, Drummond RD, Felix JM, Duarte MP, Ramiro D, Maluf MP, Sogayar MC, Menossi M (2005) Isolation and characterization of *Coffea* genes induced during coffee leaf miner (*Leucoptera coffeella*) infestation. Plant Sci 169:351–360

Murashige T, Skoog F (1962) A revised medium for rapid growth and biossays with tobacco tissue culture. Physiol Plant 15:471–497

Murdock LL, Shade RE (2002) Lectins and proteinase inhibitors as plant defenses against insects. J Agric Food Chem 50:6605–6611

Musser RO, Hum-Musser SM, Eichenseer H, Peiffer M, Ervin G, Murphy JB, Felton GW (2002) Herbivory: caterpillar saliva beats plant defenses. Nature 416:599–600

Nicholas KB, Nicholas HB Jr (1997) Gene doc: a tool for editing and annotating multiple sequence alignments. Distributed by the author. Available from http://www.psc.edu/biomed/genedoc

Oliva ML, Sampaio UM (2008) Bauhinia Kunitz-type proteinase inhibitors: structural characteristics and biological properties. Biol Chem 389:1007–1013

Onesti S, Brick P, Blow DM (1991) Crystal structure of a Kunitz-type trypsin inhibitor from *Erythrina caffra* seeds. J Mol Biol 217:153–176

Paladino A, Costantini S, Colonna G, Facchiano AM (2008) Molecular modeling of miraculin: structural analyses and functional hypotheses. Biochem Biophys Res Commun 367:26–32

Pompermayer P, Lopes AR, Terra WR, Parra JRP, Falco MC, Silva-Filho MC (2001) Effects of soybean proteinase inhibitor on development, survival and reproductive potential of the sugarcane borer, *Diatraea saccharalis*. Entomol Exp Appl 99:79–85

Ravichandran S, Dasgupta J, Chakrabarti C, Ghosh S, Singh M, Dattagupta J (2001) The role of Asn14 in the stability and conformation of the reactive-site loop of winged bean chymotrypsin inhibitor: crystal structures of two point mutants Asn14–>Lys and Asn14–>Asp. Protein Eng 14:349–357

Rawlings ND, Tolle DP, Barrett AJ (2004) MEROPS: the peptidase database. Nucleic Acids Res 32 (Database issue):D160–D164

Reymond P, Weber H, Damond M, Farmer EE (2000) Differential gene expression in response to mechanical wounding and insect feeding in *Arabidopsis*. Plant Cell 12:707–720

Rodrigues-Macedo ML, Machado Freire MG, Cabrini EC, Toyama MH, Novello JC, Marangoni S (2003) A trypsin inhibitor from *Peltophorum dubium* seeds active against pest proteinases and its effect on the survival of *Anagasta kuehniella* (Lepidoptera: Pyralidae). Biochim Biophys Acta 1621:170–182

Ryan CA (1990) Protease inhibitors in plants: genes for improving defenses against insects and pathogens. Annu Rev Phytopathol 28:425–449

Sali A, Blundell TL (1993) Comparative protein modeling by satisfaction of spatial restraints. J Mol Biol 234:779–815

Sambrook J, Fritsch EF, Maniatis T (1989) Molecular cloning: a laboratory manual, 2nd edn. Cold Spring Harbor Laboratory, Cold Spring Harbor, NY

Saraste M, Sibbald PR, Wittinghofer A (1990) The P-loop—a common motif in ATP- and GTP-binding proteins. Trends Biochem Sci 15:430–434

Shapiro AM, DeVay JE (1987) Hypersensitivity reaction of *Brassica nigra* L (Cruciferae) kills eggs of Pieris butterflies (Lepidoptera: Pieridae). Oecologia 71:631–632

Shatters RG Jr, Bausher MG, Hunter WB, Chaparro JX, Dang PM, Niedz RP, Mayer RT, McCollum TG, Sinisterra X (2004) Putative proteinase inhibitor gene discovery and transcript profiling during fruit development and leaf damage in grapefruit (*Citrus paradisi* Macf.). Gene 326:77–86

Song HK, Suh SW (1998) Kunitz-type soybean trypsin inhibitor revisited: refined structure of its complex with porcine trypsin reveals an insight into the interaction between a homologous inhibitor from *Erythrina caffra* and tissue-type plasminogen activator. J Mol Biol 275:347–363

Sumikawa JT, Brito MV, Macedo ML, Uchoa AF, Miranda A, Araujo AP, Silva-Lucca RA, Sampaio MU, Oliva ML (2010) The defensive functions of plant inhibitors are not restricted to insect enzyme inhibition. Phytochemistry 71:214–220

Tamura K, Dudley J, Nei M, Kumar S (2007) MEGA4: molecular evolutionary genetics analysis (MEGA) software version 4.0. Mol Biol Evol 24:1596–1599

Thaler JS, Bostock RM (2004) Interactions between abscisic-acid-mediated responses and plant resistance to pathogens and insects. Ecology 85:48–58

Theerasilp S, Kurihara Y (1988) Complete purification and characterization of the taste-modifying protein, miraculin, from miracle fruit. J Biol Chem 263:11536–11539

Thompson JD, Higgins DG, Gibson TJ (1994) CLUSTAL W: improving the sensitivity of progressive multiple sequence alignment through sequence weighting, position-specific gap penalties and weight matrix choice. Nucleic Acids Res 22:4673–4680

Tsukuda S, Gomi K, Yamamoto H, Akimitsu K (2006) Characterization of cDNAs encoding two distinct miraculin-like proteins and stress-related modulation of the corresponding mRNAs in *Citrus jambhiri* lush. Plant Mol Biol 60:125–136

Vallee F, Kadziola A, Bourne Y, Juy M, Rodenburg KW, Svensson B, Haser R (1998) Barley alpha-amylase bound to its endogenous protein inhibitor BASI: crystal structure of the complex at 1.9 A resolution. Structure 6:649–659

van Doorn WG, Woltering EJ (2005) Many ways to exit? Cell death categories in plants. Trends Plant Sci 10:117–122

Wagstaff C, Leverentz MK, Griffiths G, Thomas B, Chanasut U, Stead AD, Rogers HJ (2002) Cys proteinase gene expression and proteolytic activity during senescence of *Alstroemeria* petals. J Exp Bot 53:233–240

Wu HM, Cheun AY (2000) Programmed cell death in plant reproduction. Plant Mol Biol 44:267–281

Xu FX, Chye ML (1999) Expression of Cys proteinase during developmental events associated with programmed cell death in brinjal. Plant J 17:321–327

Xu ZF, Qi WQ, Ouyang XZ, Yeung E, Chye ML (2001) A proteinase inhibitor II of *Solanum americanum* is expressed in phloem. Plant Mol Biol 47:727–738